Science Bulletin 64 (2019) 1780–1787

Contents lists available at ScienceDirect

Science Bulletin

journal homepage: www.elsevier.com/locate/scib

Article

Low-cost and high safe manganese-based aqueous battery for grid energy storage and conversion

Jianhang Huang [a,c], Zhaowei Guo [a], Xiaoli Dong [a], Duan Bin [a], Yonggang Wang [a,*], Yongyao Xia [a,b,*]

[a] Department of Chemistry and Shanghai Key Laboratory of Molecular Catalysis and Innovative Materials, Institute of New Energy, iChEM (Collaborative Innovation Center of Chemistry for Energy Materials), Fudan University, Shanghai 200433, China
[b] Key Laboratory of the Ministry of Education for Advanced Catalysis Materials, Department of Chemistry, Zhejiang Normal University, Jinhua 321004, China
[c] School of Materials Science and Engineering, Nanchang Hangkong University, Nanchang 330063, China

ARTICLE INFO

Article history:
Received 2 August 2019
Received in revised form 8 September 2019
Accepted 11 September 2019
Available online 19 September 2019

Keywords:
Manganese dioxide
Copper electrode
Aqueous battery
Decoupled hydrogen evolution
Water splitting
Large-scale energy storage

ABSTRACT

As an effective energy storage technology, rechargeable batteries have long been considered as a promising solution for grid integration of intermittent renewables (such as solar and wind energy). However, their wide application is still limited by safety issue and high cost. Herein, a new battery chemistry is proposed to satisfy the requirements of grid energy storage. We report a simple Cu-Mn battery, which is composed of two separated current collectors in an H_2SO_4-$CuSO_4$-$MnSO_4$ electrolyte without using any membrane. The Cu-Mn battery shows an energy density of 40.8 Wh L^{-1}, a super-long life of 10,000 cycles (without obvious capacity decay) and negligible self-discharge. And the capital cost of US\$ 11.9 kWh^{-1} based on electrolyte is lower than any previous batteries. More importantly, the battery can still work smoothly during thermal abuse test and drill-through test, showing high safe nature. Furthermore, a combination system integrating the Cu-Mn battery and hydrogen evolution is also proposed, which is able to avoid the generation of explosive H_2/O_2 mixture, and presents an efficient approach for grid energy storage and conversion.

1. Introduction

With the constant development of electrification of the society, the generation and storage/conversion of the electric power are playing an increasing important role in our daily life. But the growing fossil consumption for the generation of electric power and the consequent ever-worsening pollution of environment make it urgent to develop clean and efficient renewable energy resource, such as solar, wind and tidal energy. As an effective technology for energy storage/conversion, rechargeable batteries possess the ability to integrate renewable energy sources with electrical grid smoothly [1,2]. Up to now, some batteries have been considered as the candidates for the applications of large-scale energy storage, e.g. Li-ion, lead-acid, redox-flow, sodium-beta alumina membrane batteries [2]. However, their wide application is still limited by safety issue and high cost [2–6]. After extensive exploration on cheap batteries [7–18], several new batteries were reported recently with the low cost potential, such as the lithium–antimony liquid metal battery (US\$ 65 kWh^{-1} based on electrode materials) [7] and the inorganic–organic flow battery (US\$ 27 kWh^{-1} based on electrode materials) [8]. However, the high operating temperature of liquid metal battery or the ion-exchange membrane in the inorganic–organic flow battery results in much additional operation and maintenance cost. And the achieve cycle life of above batteries is inferior to current Li-ion and all-vanadium redox flow batteries. So there is still a way to go in exploiting battery system with lower cost and longer cycle life.

Manganese dioxide (MnO_2) that characterized by earth abundance, low cost and environmental benignity has been widely used as the electrode active material for batteries. Over the past years, the cations (i.e., H^+, Zn^{2+} and Li^+) interaction/de-interaction reactions of MnO_2 coupled with the valence state change between Mn^{4+} and Mn^{3+} have been employed to build various low cost batteries, including rechargeable Zn-MnO_2 battery with a neutral electrolyte [19–22] and Li-ion battery (e.g., $LiMn_2O_4$ as cathode material) with non-aqueous [23–27] and aqueous electrolyte [28,29]. However, these batteries generally suffer from the limited cycle life due to the structure collapse of MnO_2 and the dissolution of Mn^{2+} (from Mn^{3+} disproportionation) [21–24]. Fortunately, manganese can exist in various valence states (e.g., Mn^0, Mn^{2+}, Mn^{3+}, Mn^{4+} and Mn^{7+}), which thus enable us to design new manganese-based battery chemistry. For example, Chen et al. [30] recently reported a long-life H_2-Mn battery using acid

---

[*] Corresponding authors.
E-mail addresses: ygwang@fudan.edu.cn (Y. Wang), yyxia@fudan.edu.cn (Y. Xia).

https://doi.org/10.1016/j.scib.2019.09.020
2095-9273/

electrolyte, which depends on the electrochemical deposition/dissolution of MnO_2 in positive electrode and the H_2 evaluation/reduction reaction (HER/HRR) in negative electrode. However, the expensive catalysts for HER/HRR and the complex H_2 storage technology much increase the cost and safety risk of the H_2-Mn battery. Especially, the crossover of H_2 results in obvious self-discharge. And the flammable H_2 sealed in battery is dangerous to large-scale application for energy storage. Replacing the hydrogen with metal electrode (such as Cu) to form metal-manganese battery might be a practicable idea, which has been patented by our group in 2018 [31]. Very recently, several groups investigated this Cu-Mn battery [32,33]. However, the achieved performances, such as the low areal capacity (<1 mAh cm^{-2}) and limited cycle life (<2000 cycles), are still far away from practical application.

Herein, we demonstrate a Cu-Mn battery chemistry, which contains the electro-active species (Mn^{2+} and Cu^{2+}) in an dilute acid electrolyte (H_2SO_4) and two separated current collectors for positive and negative electrodes (e.g., carbon felt and copper plate, Fig. S1 (online)). Its charge involves the electrochemical deposition of MnO_2 ($Mn^{2+} + 2H_2O - 2e^- \rightarrow MnO_2\downarrow + 4H^+$) in positive electrode (the areal deposition capacity can reach up to 50 mAh cm^{-2}) and the Cu plating ($Cu^{2+} + 2e^- \rightarrow Cu\downarrow$) on negative electrode, which is in parallel with the electrons transfer from positive to negative electrode via out circuit. Discharge reverses the charge. When calculated based on the H_2SO_4-$CuSO_4$-$MnSO_4$ electrolyte, the demo battery exhibits a low cost of US$ 11.9 kWh^{-1} and a competitive energy density of 40.8 Wh L^{-1}, which is comparable to that of all-vanadium redox flow battery. Meanwhile, the battery can still work smoothly during thermal abuse test and drill-through test, showing high safe nature. The simple structure, inherent low cost, high safety and promising performance enable the Cu-Mn battery to possess a bright application prospect on grid energy storage. Furthermore, we integrated the Cu-Mn battery and hydrogen evolution process into a combined system to producing hydrogen and electric energy alternately. This system eliminates the explosive H_2/O_2 mixture in traditional water electrolysis, and replaces the worthless oxygen with electric energy, which may provide a possible approach to utilize renewable effectively.

2. Materials and methods

2.1. Materials

All materials were used as received: Copper(II) sulfate pentahydrate ($CuSO_4 \cdot 5H_2O$, AR), Manganese(II) sulfate monohydrate ($MnSO_4 \cdot H_2O$, AR), Sulfuric acid (H_2SO_4, AR), Copper plate (Cu, thickness of 0.1 mm). Above reagents were brought from Sinopharm Chemical Reagent Co., Ltd; Carbon felt (thickness of 5 mm) was brought from Dalian Longtian Tech. Co., Ltd; the HER electrode was purchased from Baoji Zhiming Special Metal Co., Ltd.

2.2. Electrochemical measurements

Electrochemical measurements for Cu-Mn battery were performed with flooded cells, in which a solution of 0.5 mol L^{-1} H_2SO_4 + 0.8 mol L^{-1} $CuSO_4$ + 0.8 mol L^{-1} $MnSO_4$, carbon felt (1 cm^2 area and 5 mm thickness) and Cu plate (1 cm^2 area and 0.1 mm thickness) were used as electrolyte, positive collector and negative collector, respectively. The charge/discharge perfor-

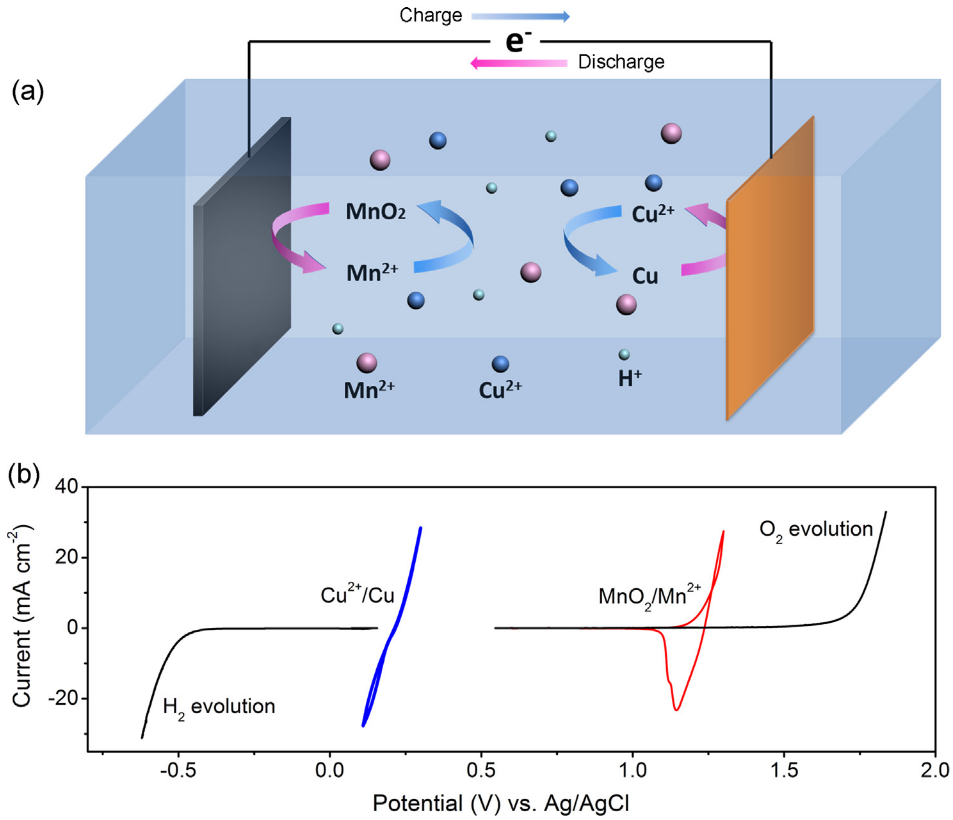

Fig. 1. (Color online) Working principle of the Cu-Mn cell. (a) The schematic illustration of the Cu-Mn cell during charge/discharge process. The charge process involves electrochemical deposition of MnO_2 in positive electrode and the Cu plating on negative electrode, which is in parallel with the electrons transfer from positive to negative electrode via out circuit. Discharge reverses the charge. (b) CV of MnO_2/Mn^{2+} (red curve) and Cu^{2+}/Cu (blue curve) in the electrolyte containing 0.5 mol L^{-1} H_2SO_4 + 0.8 mol L^{-1} $CuSO_4$ + 0.8 mol L^{-1} $MnSO_4$ at a sweep rate of 1 mV s^{-1}; LSV of oxygen evolution reaction (OER) on carbon felt, and LSV of HER on Cu plate in the electrolyte containing 0.5 mol L^{-1} H_2SO_4 at a sweep rate of 1 mV s^{-1}.

mances, cyclic voltammetry (CV) and linear sweep voltammetry (LSV) were conducted on an electrochemical workstation (BioLogic VSP-300) and battery test system (Neware CT-9004). The HER cell consists of Pt-coated Ti-mesh electrode (1 cm^2) as HER electrode, carbon felt (1 cm^2) as cathode, and 1 mol L^{-1} $MnSO_4$ + 0.5 mol L^{-1} H_2SO_4 electrolyte. The Cu-Mn cell consists of Cu palte (1 cm^2), 0.5 mol L^{-1} H_2SO_4 electrolyte, the carbon felt in HER cell is used as cathode for Cu-Mn cell. In Step 1, the HER cell is charged under 1.5 V to 1 mAh cm^{-2}, then the MnO_2 electrode is moved to the Cu-Mn cell. In Step 2, the Cu-Mn cell discharges at 10 mA cm^{-2} to 0.3 V. Repeating Step 1 and Step 2 alternatively, hydrogen and electric energy will produce alternatively.

2.3. Material characterization

X-Ray diffraction (XRD) patterns were collected on an X-ray diffractometer (Bruker D8 Advance, Germany) with Cu Kα radiation (λ = 0.15406 nm). Scanning electron microscope (SEM) images were obtained on field-emission JEOL JSM-6390 microscope. X-ray photoelectron spectroscopy (XPS) was tested on a Thermo Escalab 250 equipped with a hemispherical analyzer.

2.4. Cost estimation

The main cost of the Cu-Mn cell is $CuSO_4 \cdot 5H_2O$, $MnSO_4 \cdot H_2O$ and H_2SO_4. And the average price of $CuSO_4 \cdot 5H_2O$ and $MnSO_4 \cdot H_2O$ (electroplating grade) is US$ 2 and 0.55 kg^{-1} respectively, and 98% H_2SO_4 is US$ 0.2 kg^{-1}, which was obtained from www.alibaba.com. The cost of the cell is calculated according to the following equation: $P = \sum_i p_i m_i / E$, where P is the capital cost per unit of discharged electrical energy (US$ kWh^{-1}), p_i is the cost per unit of metal salt used in electrolyte (US$ kg^{-1}), m_i is the mass of metal salt (kg), and E is the discharged energy of the cell (kWh), which is obtained from the demo Cu-Mn battery. And the detailed calculation is presented in Table S1 (online).

3. Results and discussion

The structure and operation principle of the Cu-Mn battery is schematically illustrated in Fig. 1a. As shown in Fig. 1a, Mn^{2+} in the electrolyte is oxidized into MnO_2 during the charge process, which is deposited on the positive collector (carbon felt). Meanwhile, Cu^{2+} in the electrolyte is reduced into metal Cu, which is deposited on the negative collector (Cu plate). As to discharge process, the MnO_2 deposited on the carbon felt is reduced to Mn^{2+} and dissolve into electrolyte. In the meantime, metal Cu is oxidized to Cu^{2+} and dissolved into electrolyte. Due to the inherent deposition/dissolution of active species, the Cu-Mn battery no longer needs an ion permselective membrane to separate anolyte and catholyte, and no need to prepare active materials. The corresponding electrode reactions are described as follow:

$$\text{Cathode: } Mn^{2+} + 2H_2O \leftrightarrow MnO_2\downarrow + 4H^+ + 2e^- \quad (1)$$

$$\text{Anode: } Cu^{2+} + 2e^- \leftrightarrow Cu\downarrow \quad (2)$$

$$\text{Overall: } Mn^{2+} + Cu^{2+} + 2H_2O \leftrightarrow MnO_2\downarrow + Cu\downarrow + 4H^+ \quad (3)$$

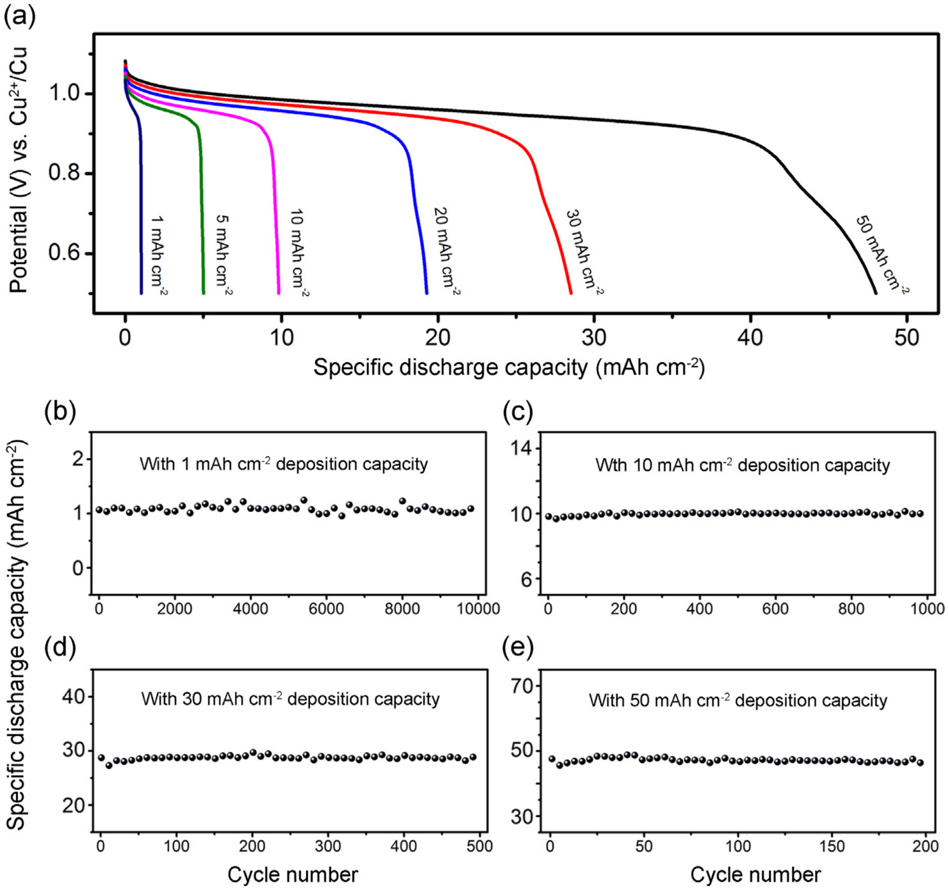

Fig. 2. (Color online) Electrochemical performance of the Cu-Mn cell. (a) The 1th cycle discharge profiles of the cells with different deposition capacities (i.e., the charge capacities). The cell is charged under 1.2 V to 1–50 mAh cm^{-2} respectively, and discharged at 10 mA cm^{-2} to 0.5 V. Cycle performance of the cell with deposition capacity of 1 mAh cm^{-2} (b), 10 mAh cm^{-2} (c), 30 mAh cm^{-2} (d) and 50 mAh cm^{-2} (e), respectively, which are charged under 1.2 V and discharged at 10 mA cm^{-2} to 0.5 V. The average Coulombic efficiencies for the battery with 1, 10, 30 and 50 mAh cm^{-2} deposition capacity are 101.2%, 99.7%, 95.6% and 94.6% respectively.

Prior to the fabrication of the battery, the redox potentials of MnO_2/Mn^{2+} and Cu^{2+}/Cu were determined by CV tests, which is compared with the oxygen/hydrogen evolution potentials obtained by LSV. As we can see in Fig. 1b, the redox potential of MnO_2/Mn^{2+} is lower than oxygen evolution. Meanwhile, the redox potential of Cu^{2+}/Cu is higher than hydrogen evolution, indicating that the Cu-Mn cell is feasible in aqueous electrolyte without the oxygen and hydrogen evolution.

In order to demonstrate the hypothesis shown in Fig. 1a, we fabricated a prototype flooded cell, which contains a positive collector (a piece of carbon felt with area of 1 cm^2 and thickness of 5 mm), a negative collector (a piece of copper plate with area of 1 cm^2 and thickness of 0.1 mm), and a dilute acid aqueous electrolyte (0.5 mol L^{-1} H_2SO_4, 0.8 mol L^{-1} $CuSO_4$ and 0.8 mol L^{-1} $MnSO_4$). The assembled cell is in the discharged state, which needs to be charged first. And a constant-voltage charging technique is applied due to its smooth discharge profile (Fig. S2 online). The cells were charged under a constant voltage of 1.2 V with the charge capacities (i.e., the deposition capacities) of 1, 5, 10, 20, 30 and 50 mAh cm^{-2}, respectively. The corresponding charge current profiles of 50 mAh cm^{-2} under constant 1.2 V are shown in Fig. S3 (online), where it can be observed that the charge current can reach the maximum of ~100 mA cm^{-2}, endowing the cell with flexible adjustability for high current input from the renewable energy. For example, it only needs 38 s to charge to 1 mAh cm^{-2}, and 41.2 min to 50 mAh cm^{-2}. After charging, these cells were discharged at 10 mA cm^{-2} with a cut-off voltage of 0.5 V. The discharge profiles of these cells with different deposition capacities are given in Fig. 2a. It can be seen that the average discharge platform is around 0.96 V. The Coulombic efficiencies are 102.7%, 100%, 98.2%, 96.4%, 95.1% and 96.0% according to the deposition capacities of 1, 5, 10, 20, 30 and 50 mAh cm^{-2}, respectively (the > 100% Coulombic efficiency can be ascribed to the electrochemical double-layer capacitance of carbon felt current collectors with high surface area [30]). And the corresponding energy efficiencies are 81.7%, 79.2%, 77.5%, 75.7%, 74.0% and 73.7%, respectively. Although there is a decrease of energy efficiency with the increase of deposition capacity of MnO_2, the energy efficiency is still above 70% when the deposition capacity reaches up to 50 mAh cm^{-2}, indicating a high energy utilization of the cell. Fig. 2b–e shows the cycle performance of the Cu-Mn cells tested with different deposition capacities. It can be detected that there is no obvious decay on discharge capacity over 10,000 cycles for the cell with a low deposition capacity of 1 mAh cm^{-2} (Fig. 2b), showing an excellent cyclic stability (which is five times longer than 2000 cycles under 0.8 mAh cm^{-2} capacity reported in Ref. [33]). When charged with the higher deposition capacities of 10 and 30 mAh cm^{-2}, the Cu-Mn cells also keep very stable discharge capacity during 1000 and 500 cycles (Fig. 2c and d). Even with a very high deposition capacity of 50 mAh cm^{-2}, the Cn-Mn cell still shows stable discharge capacities over 200 cycles (Fig. 2e). Furthermore, its discharge profiles are almost unchangeable during 200 cycles (Fig. S4 online), which demonstrates that the carbon felt possesses a great reversibility under high deposition capacity of MnO_2. Element analysis confirms that MnO_2 is the main production of the deposition process (Fig. S5 online). And the *ex-situ* XRD, XPS and SEM characterization (Fig. S6 online) further prove the high reversibility of MnO_2/Mn^{2+} redox. On the other hand, Cu anode also shows high reversibility with Coulombic efficiency around 99% (Fig. S7 online).

Rate capability is one of the most important evaluations for reversible battery, and the rate capabilities of these Cu-Mn cells with different deposition capacities are presented in Fig. 3. The Cu-Mn cells were charged at 1.2 V to the capacities of 1, 10, 30,

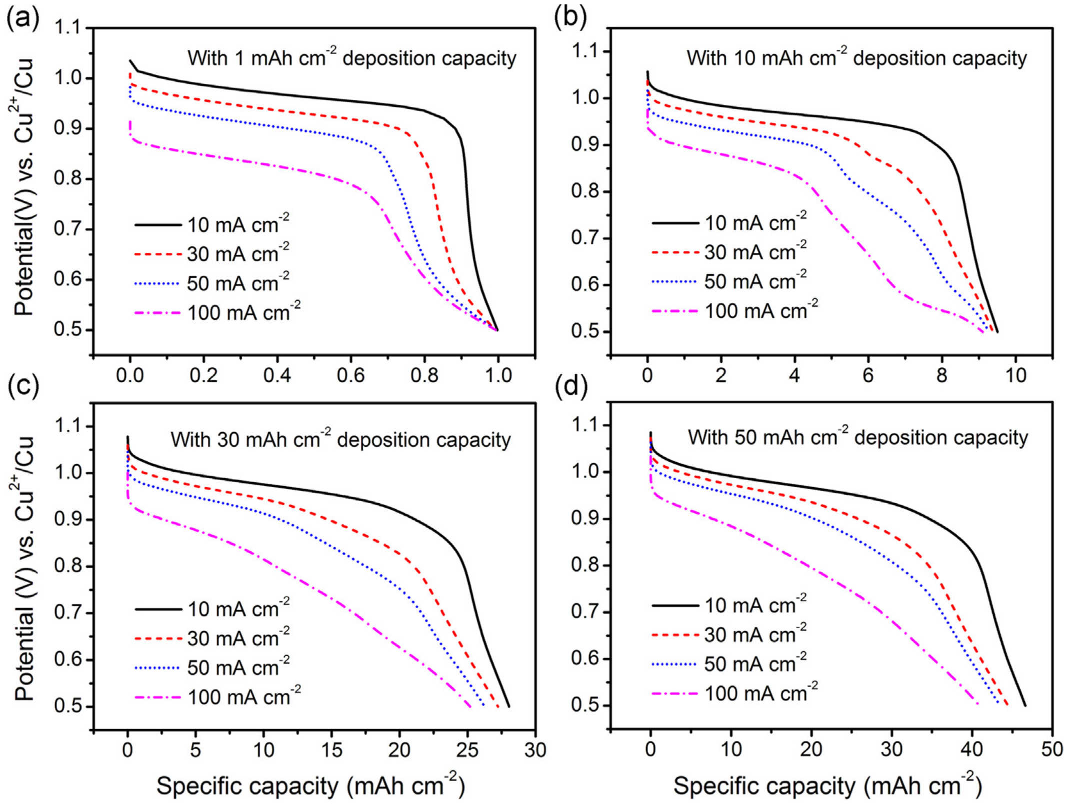

Fig. 3. (Color online) Rate performance of the Cu-Mn cells with different deposition capacities. The discharge profiles at different currents of the Cu-Mn cells with various deposition capacities (i.e., charge capacities) of 1 mAh cm^{-2} (a), 10 mAh cm^{-2} (b), 30 mAh cm^{-2} (c) and 50 mAh cm^{-2} (d), respectively. In this experiment, these cells are charged to a certain capacities (1, 10, 30 and 50 mAh cm^{-2}, respectively), and each cell is discharged at different currents (10, 30, 50 and 100 mA cm^{-2}) to 0.5 V.

50 mAh cm^{-2}, respectively. And each of them discharged at ever-increasing current densities ranging from 10 to 100 mA cm^{-2}. Although there are some voltage losses at high applied current densities (Fig. 3), all of these Cu-Mn cells can endure the high discharge current density of 100 mA cm^{-2} and exhibit excellent capacity retentions. For the Cu-Mn cell with a deposition capacity (i.e., charge capacity) of 1 mAh cm^{-2}, there is no capacity loss with the increasing discharge currents (Fig. 3a), which is beneficial from the fast kinetics of redox of Mn^{2+}/MnO_2 and Cu^{2+}/Cu in dilute acid electrolyte. When the deposition capacity of the Cu-Mn cell is increased to 10 mAh cm^{-2}, only a slight capacity loss emerges with increase of discharge current (Fig. 3b). With the further increase of deposition capacities to 30 and 50 mAh cm^{-2}, the Cu-Mn cells only show a small amount of capacity losses at the high applied current of 100 mA cm^{-2} (Fig. 3c, d), indicating that the plenty MnO_2 deposition do not cause sharp deterioration of discharge performance at high current density. As to large-scale energy storage, the self-discharge performance is an important consideration to prevent energy loss during storage. So the self-discharge performance with deposition capacity of 50 mAh cm^{-2} is investigated. Fig. S8a (online) shows the discharge curves without and with open circuit voltage (OCV) measurement. After 100 h OCV measurement (the change of OCV during rest is given in Fig. S8b (online)), the average operating voltage decrease to 0.9 V, showing 60 mV lower than 0.96 V for the cell without OCV measurement. But impressively, the capacity loss is only 0.7%, i.e., capacity retention of 99.3%. And the corresponding energy retention is 91.9% compared with sample without self-discharge test. The self-discharge performance is much superior than Manganese-Hydrogen cell (71% remaining capacity after 80 h) [30]. The relative low capacity loss can be ascribed to the fact that the MnO_2 is stable in the aqueous electrolyte, which endows the Cu-Mn cell with immense superiority in the field of large-scale energy storage.

The simple structure and high electrochemical performance of the Cu-Mn cell motivate us to scale up the battery system, and two approaches are developed in terms of voltage and capacity, respectively. First, a 3 V Cu-Mn battery in series connection is assembled towards high voltage Cu-Mn battery. The inset of Fig. 4a shows the structural representation of the 3 V Cu-Mn battery (the photograph of the assembled battery is shown in Fig. S9a (online)), in which the area of carbon felt is 12 cm^2 and 5 mm thickness. Only simple stack of the three single cells is needed to obtain higher voltage. The battery is charged under 3.6 V to 60, 120 and 360 mAh, respectively, and then discharged at 30 mA to the cut-off voltage of 1.5 V. Fig. 4a shows the discharge profiles with different deposition capacities. It can be seen that the average operating voltage is around 3 V, which is three times higher than that of the single Cu-Mn cell. And the discharge capacity is 57.2, 113.3 and 331.7 mAh, according to the Coulombic efficiency of 95.3%, 94.4% and 92.1% based on the deposition capacity of 60, 120, 360 mAh. And there is no obvious capacity decay after 50 cycles at deposition capacity of 120 mAh (Fig. S9b online). Furthermore, a 4 V Cu-Mn battery using four single cells are assembled to power an electric toy car (Video S1 (online)), the toy car requires a power ~2 W), indicating that the Cu-Mn battery possess a good ability of high power output.

Second, a 1 V 6.2 Ah demo battery is constructed to demonstrated the easy scalability of battery capacity (Fig. S10 online). As shown in the structural representation of the demo battery (inset of Fig. 4b), it contains 155 mL electrolyte (0.5 mol L^{-1} H_2SO_4 + 0.8 mol L^{-1} $CuSO_4$ + 0.8 mol L^{-1} $MnSO_4$) and four pieces of carbon felt (30 cm^2 and 5 mm thickness for each pieces). The demo battery is charged under 1.2 V to 1000, 3000 mAh and the theoretical capacity of 6646 mAh, respectively, and discharged at 100 mA to the cut-off voltage of 0.5 V. Fig. 4b shows the discharge profiles of the demo battery at different deposition capacities. It can be seen that the Coulombic efficiency is 97.4% and 96.2% at 1000 mAh and 3000 mAh. Even the deposition capacity (i.e., charge capacity) reaches theoretical value of 6646 mAh, the Cu-Mn battery can exhibits a discharge capacity of 6285 mAh with a high 94.6% Coulombic efficiency, indicating the high electrolyte utilization. Furthermore, there is no obvious capacity decay after 50 cycles at deposition capacity of 1000 mAh (Fig. S10b online).

The energy density and the cost estimation of the Cu-Mn system are based on the above mentioned 1 V, 6.2 Ah demo battery. The actual discharge energy of the demo battery is 6325 mWh, according to 79.3% energy utilization (charge energy is 7975 mWh). And the energy density is 40.8 Wh L^{-1}/33.5 Wh kg^{-1} (based on the 155 mL electrolyte containing 0.5 mol L^{-1} H_2SO_4, 0.8 mol L^{-1} $CuSO_4$ and 0.8 mol L^{-1} $MnSO_4$). Furthermore, the total mass of the demo battery (including electrolyte, current collectors and battery shell) is 310 g, according to the 20.4 Wh kg^{-1} for the whole demo battery, which is comparable to the conventional flow batteries, such as all-vanadium redox flow battery [34,35]. The main cost of the Cu-Mn battery is the electrolyte containing $CuSO_4$, $MnSO_4$ and H_2SO_4. And their costs are given in Table S1 (online), from which the capital cost of US$ 11.9 kWh^{-1} is calculated based on the electrolyte, the detailed calculation is shown in methods

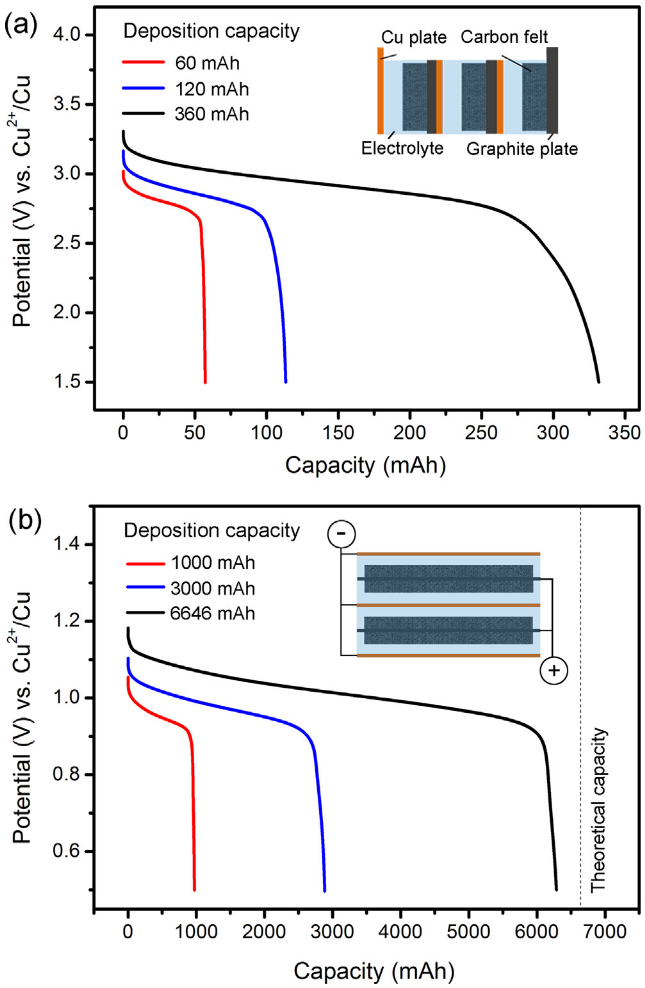

Fig. 4. (Color online) Scale-up of the Cu-Mn cell. The discharge profiles of the 3 V Cu-Mn battery (a) and 1 V, 6.2 Ah demo battery (b) with different deposition capacities. The schematic illustrations of the battery structure are given in the inset of figures. The 3 V batteries are charged under 3.6 V to 60, 120, 360 mAh respectively, and discharged at 30 mA to 1.5 V. The 1 V, 6.2 Ah demo batteries are charged under 1.2 V to 1000, 3000, 6646 mAh respectively, and discharged at 100 mA to 0.5 V.

section and Table S1 (online). It is much lower than that of any previous batteries reported (Table S2 online) [2,7,8].

Battery safety is the most important consideration towards the grid energy storage. So the safety testing of the demo battery is conducted here, which contains thermal abuse testing and drill-through testing. For the thermal abuse testing, the demo battery is charged to 6 Ah first, and toasted with the open flame. From Video S2 (online) we can see that the demo battery has no risk of explosion when exposed to intense heat. Furthermore, it still works well during toast testing, demonstrating the excellent safety and reliability. In addition, Video S3 (online) shows the drill-through testing of the demo battery which was pre-charged to 6 Ah. As expected, there is no explosion, just electrolyte leakage during testing. And as long as there is electrolyte maintained in the battery, it can work well during drill-through. Above tests demonstrate the high safety of Cu-Mn battery under some extreme conditions.

Interestingly, due to the excellent reversibility of MnO_2/Mn^{2+} redox, the Cu-Mn system not only can be utilized as rechargeable battery, but also can be combined with hydrogen evolution to make full use of renewable energy. The working principle is presented in Fig. 5. In Step 1 for hydrogen evolution (Fig. 5a), when a voltage is applied between the HER electrode and carbon felt electrode, H^+ is reduced to hydrogen on HER electrode, and Mn^{2+} is oxidized to MnO_2 along with the production of H^+ on carbon felt electrode. Subsequently, in Step 2 (Fig. 5b), the MnO_2 formed in Step 1 is coupled with Cu anode to form a Cu-Mn cell to provide electricity, in which the MnO_2 is reduced to Mn^{2+}, and Cu is oxidized to Cu^{2+} (Noted that Cu electrode is just used here for a demonstration of the combination system concept, it can be replaced by other electrodes, such as zinc electrode). Fig. 5c shows the voltage profiles for Step 1 (HER cell, left part with pink color) and Step 2 (Cu-Mn cell, right part with nattier blue color), and the corresponding current are shown in Fig. S11 (online). With the Step 1 and Step 2 running alternately, hydrogen and electric energy can be produced alternately. Note that the oxidation of Cu can be substituted by others oxidation process with high added-value, such as oxidation of ethanol, benzyl alcohol, furfural and so on.

From above discussion, it can be concluded that the Cu-Mn battery possessed some advantages. First, the components of the cell are low cost. More importantly, there is no need of membrane, catalysts, harsh gas-tight requirement and high operating temperature, which gives considerable design flexibility and low maintenance cost. For example, cylinder-type, pouch-type, prismatic-type and flow-assisted Cu-Mn battery (Fig. S12 online) are attractive for the further investigation. The low capital cost (US$ 11.9 kWh^{-1}) and the ease of fabrication make the Cu-Mn cell to be a great potential candidate for large-scale energy storage; Second, due to the nonflammable materials (including electrolyte and current collectors, and the non-combustibility test for carbon felt is shown in Video S4 (online)), the battery shows high safety

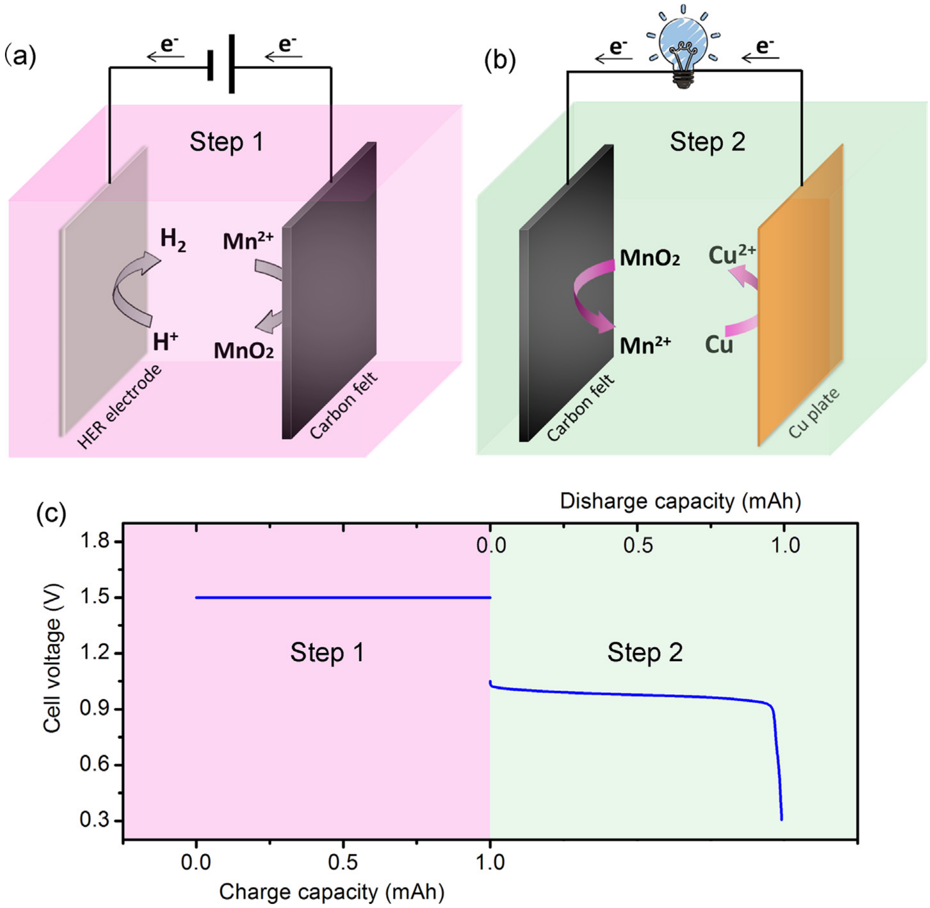

Fig. 5. (Color online) Demonstration of the combination system between Cu-Mn cell and hydrogen evolution. (a) The HER cell consists of HER electrode (Pt-coated Ti-mesh electrode, 1 cm^2), carbon felt (1 cm^2) and 1 mol L^{-1} $MnSO_4$ + 0.5 mol L^{-1} H_2SO_4 electrolyte. (b) The Cu-Mn cell consists of Cu palte (1 cm^2) and 0.5 mol L^{-1} H_2SO_4 electrolyte. (c) The applied constant voltage of 1.5 V for HER in Step 1 (pink part on the left), and the discharge voltage for Cu-Mn cell (blue curve) in Step 2 at 10 mA cm^{-2} current (nattier blue part on the right). For Step 1, HER cell is charged, which involves HER process and electrochemical deposition of MnO_2 on carbon felt. For Step 2, the carbon felt with deposited MnO_2 and Cu plate form Cu-Mn cell to deliver electric energy. With the alternation between Step 1 and Step 2, hydrogen and electric energy will produce alternately.

during thermal abuse and drilling-through testing. In addition, there is no gas evolution during the cycling, eliminating the explosion caused by high-pressure gas or flammable gas; Third, the durable carbon felt with strong affordability on massive MnO_2 deposition guarantee the long cycle life and high discharge capacity. Meanwhile, the proposed battery shows excellent capacity retention in self-discharge test.

4. Conclusion

In summary, we proposed a simple Cu-Mn battery based on the deposition/dissolution of MnO_2 and Cu in aqueous solution. And the feasibility of scale-up and high safety is demonstrated by some demo batteries. The low solubility of $CuSO_4$ limits the energy density of the system. But it can be enhanced by optimizing the composition of electrolyte, such as substituting $CuSO_4$ with others Cu salt with high solubility. And it should be aware that the battery performance can be further improved by the optimization of electrolyte and structure design of electrode. The low cost, high safety and high cycling stability of the battery system sheds light on the production of safe, reliable and economical large-scale energy storage system. In addition, a combination system integrating the HER and Cu-Mn cell are presented, which may shed light on the flexible design and application of large-scale energy storage and conversion.

Conflict of interest

The authors declare that they have no conflict of interest.

Acknowledgments

This work was financially supported by the National Natural Science Foundation of China (21622303, 21333002, 21805126), and National Key Research and Development Plan (2016YFB0901500, 2016YFA0203302).

Author contributions

Yonggang Wang conceived this idea and designed the experiments. Yonggang Wang and Yongyao Xia directed the project. Jianhang Huang and Zhaowei Guo carried out the electrochemical measurements and data analysis. Jianhang Huang, Xiaoli Dong and Duan Bin performed the battery scale-up. Jianhang Huang and Yonggang Wang co-wrote the paper. All authors discussed the results and commented on the manuscript.

Appendix A. Supplementary materials

Supplementary materials to this article can be found online at https://doi.org/10.1016/j.scib.2019.09.020.

References

[1] Larcher D, Tarascon JM. Towards greener and more sustainable batteries for electrical energy storage. Nat Chem 2015;7:19.

[2] Dunn B, Kamath H, Tarascon JM. Electrical energy storage for the grid: a battery of choices. Science 2011;334:928–35.

[3] Yang Z, Zhang J, Kintner-Meyer MC, et al. Electrochemical energy storage for green grid. Chem Rev 2011;111:3577–613.

[4] Goodenough JB. Electrochemical energy storage in a sustainable modern society. Energ Environ Sci 2014;7:14–8.

[5] Chu S, Cui Y, Liu N. The path towards sustainable energy. Nat Mater 2017;16:16–22.

[6] Soloveichik GL. Battery technologies for large-scale stationary energy storage. Annu Rev Chem Biomol Eng 2011;2:503–27.

[7] Wang K, Jiang K, Chung B, et al. Lithium-antimony-lead liquid metal battery for grid-level energy storage. Nature 2014;514:348–50.

[8] Huskinson B, Marshak MP, Suh C, et al. A metal-free organic-inorganic aqueous flow battery. Nature 2014;505:195–8.

[9] Lin KX, Chen Q, Gerhardt MR, et al. Alkaline quinone flow battery. Science 2015;349:1529–32.

[10] Chao D, Zhou W, Ye C, et al. An electrolytic Zn–MnO_2 battery for high-voltage and scalable energy storage. Angew Chem Int Edit 2019;58:7823–8.

[11] Hollas A, Wei XL, Murugesan V, et al. A biomimetic high-capacity phenazine-based anolyte for aqueous organic redox flow batteries. Nat Energy 2018;3:508–14.

[12] Zhang L, Zhang C, Ding Y, et al. A low-cost and high-energy hybrid iron-aluminum liquid battery achieved by deep eutectic solvents. Joule 2017;1:623–33.

[13] Suo LM, Borodin O, Gao T, et al. "Water-in-salt" electrolyte enables high-voltage aqueous lithium-ion chemistries. Science 2015;350:938–43.

[14] Hu P, Zhu T, Wang X, et al. Highly durable $Na_2V_6O_{16}\cdot 1.63H_2O$ nanowire cathode for aqueous zinc-ion battery. Nano Lett 2018;18:1758–63.

[15] Liang YL, Jing Y, Gheytani S, et al. Universal quinone electrodes for long cycle life aqueous rechargeable batteries. Nat Mater 2017;16:841.

[16] Mo F, Li H, Pei Z, et al. A smart safe rechargeable zinc ion battery based on sol-gel transition electrolytes. Sci Bull 2018;63:1077–86.

[17] Janoschka T, Martin N, Martin U, et al. An aqueous, polymer-based redox-flow battery using non-corrosive, safe, and low-cost materials. Nature 2015;527:78–81.

[18] Huang J, Guo Z, Ma Y, et al. Recent progress of rechargeable batteries using mild aqueous electrolytes. Small Methods 2019;3:1800272.

[19] Xu C, Li B, Du H, et al. Energetic zinc ion chemistry: the rechargeable zinc ion battery. Angew Chem Int Edit 2012;51:933–5.

[20] Zhang N, Cheng F, Liu J, et al. Rechargeable aqueous zinc-manganese dioxide batteries with high energy and power densities. Nat Commun 2017;8:405.

[21] Huang J, Wang Z, Hou M, et al. Polyaniline-intercalated manganese dioxide nanolayers as a high-performance cathode material for an aqueous zinc-ion battery. Nat Commun 2018;9:2906.

[22] Pan HL, Shao YY, Yan PF, et al. Reversible aqueous zinc/manganese oxide energy storage from conversion reactions. Nat Energy 2016;1:16039.

[23] Xia YY, Zhou YH, Yoshio M. Capacity fading on cycling of 4 V Li/$LiMn_2O_4$ cells. J Electrochem Soc 1997;144:2593–600.

[24] Zhan C, Wu TP, Lu J, et al. Dissolution, migration, and deposition of transition metal ions in Li-ion batteries exemplified by Mn-based cathodes-a critical review. Energ Environ Sci 2018;11:243–57.

[25] Park SH, Myung ST, Oh SW, et al. Ultrasonic spray pyrolysis of nano crystalline spinel $LiMn_2O_4$ showing good cycling performance in the 3 V range. Electrochim Acta 2006;51:4089–95.

[26] Jiao F, Bao J, Hill AH, et al. Synthesis of ordered mesoporous Li-Mn-O spinel as a positive electrode for rechargeable lithium batteries. Angew Chem Int Edit 2008;47:9711–6.

[27] Freire M, Kosova NV, Jordy C, et al. A new active Li-Mn-O compound for high energy density Li-ion batteries. Nat Mater 2016;15:173.

[28] Zhi J, Yazdi AZ, Valappil G, et al. Artificial solid electrolyte interphase for aqueous lithium energy storage systems. Sci Adv 2017;3:e1701010.

[29] Wang F, Borodin O, Gao T, et al. Highly reversible zinc metal anode for aqueous batteries. Nat Mater 2018;6:543.

[30] Chen W, Li G, Pei A, et al. A manganese–hydrogen battery with potential for grid-scale energy storage. Nat Energy 2018;3:428–35.

[31] Wang Y, Xia Y, Huang J. Copper-Manganese battery based on deposition/dissolution redox reaction. China Patent, CN 108428926 A.

[32] Wei L, Zeng L, Wu M, et al. An aqueous manganese-copper battery for large-scale energy storage applications. J Power Sour 2019;423:203–10.

[33] Liang G, Mo F, Li H, et al. A universal principle to design reversible aqueous batteries based on deposition–dissolution mechanism. Adv Energy Mater 2019:1901838.

[34] Cunha A, Martins J, Rodrigues N, et al. Vanadium redox flow batteries: a technology review. Int J Energy Res 2015;39:889–918.

[35] Ponce de León C, Frías-Ferrer A, González-García J, et al. Redox flow cells for energy conversion. J Power Sources 2006;160:716–32.

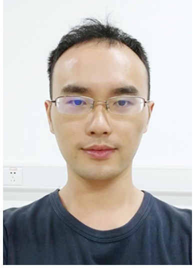

Jianhang Huang received his Ph.D. degree from Central South University in June 2015. He has been working as a lecturer at Nanchang Hangkong University since 2015. In 2017, he moved to Fudan University to complete his post-doctoral training under the supervision of Profs. Yongyao Xia and Yonggang Wang. His research focuses on aqueous energy-storage system and advanced materials for electrode and electrolyte.

Yonggang Wang received his Ph.D. degree in Physical Chemistry from Fudan University in 2007. From 2007 to 2011, he worked as a Post-doctoral Research Associate at the National Institute of Advanced Industrial Science and Technology (AIST), Japan. He is currently a full professor at the Department of Chemistry at Fudan University, China. His research interests include new energy storage & conversion system, and next generation rechargeable batteries.

Yongyao Xia is a professor in the Department of Chemistry of Fudan University. He received his Ph.D. degree in Energy-Related-Material Science in Saga University, Japan in 1997. His research interests involve advanced materials and technologies for energy storage and conversion devices, e.g., lithium-ion batteries, sodium-ion batteries, electrochemical supercapacitors and new energy storage technology.